Serial Analysis of 38 Proteins during the Progression of Human Breast Tumor in Mice Using an Antibody Colocalization Microarray*[S]

Huiyan Li‡§¶, Sébastien Bergeron‡§, Matthew G. Annis‖, Peter M. Siegel‖, and David Juncker‡§‡‡**

Proteins in serum or plasma hold great potential for use in disease diagnosis and monitoring. However, the correlation between tumor burden and protein biomarker concentration has not been established. Here, using an antibody colocalization microarray, the protein concentration in serum was measured and compared with the size of mammary xenograft tumors in 11 individual mice from the time of injection; seven blood samples were collected from each tumor-bearing mouse as well as control mice on a weekly basis. The profiles of 38 proteins detected in sera from these animals were analyzed by clustering, and we identified 10 proteins with the greatest relative increase in serum concentration that correlated with growth of the primary mammary tumor. To evaluate the diagnosis of cancer based on these proteins using either an absolute threshold (*i.e.* a concentration cutoff) or self-referenced differential threshold based on the increase in concentration before cell injection, receiver operating characteristic curves were produced for 10 proteins with increased concentration, and the area under curve was calculated for each time point based on a single protein or on a panel of proteins, in each case showing a rapid increase of the area under curve. Next, the sensitivity and specificity of individual and optimal protein panels were calculated, showing high accuracy as early as week 2. These results provide a foundation for studies of tumor growth through measuring serial changes of protein concentration in animal models. ***Molecular & Cellular Proteomics 14: 10.1074/mcp.M114.046516, 1024–1037, 2015.***

Proteins in blood have long been used as biomarkers for cancer disease management (1, 2). Proteins up-regulated in cancer cells may be found at higher concentration in blood, and their use for disease prognosis and response to therapy is well established (3). For example, CA-125 has been used as a biomarker to monitor the tumor progression and treatment response of ovarian cancer (4). The prospect of screening and diagnosing cancer based on the detection of blood-based biomarkers has generally not been fulfilled. Compared with single point detection, time course analysis of biomarkers in serially collected samples can improve the accuracy of biomarker detection, is notably used to help diagnose prostate cancer in man using prostate-specific antigen, and is widely used to evaluate progression of tumors.

Recently, Gambhir and co-workers (5, 6) proposed a mathematical model relating secreted blood biomarker levels to tumor sizes for ovarian cancer. Lutz *et al.* (5) proposed the first model with protein excretion into circulation assumed to be proportional to tumor volume and to have a fixed half-life, finding that protein concentration is linearly correlated with tumor size. Later Hori and Gambhir (6) improved the model by incorporating dynamic protein levels over time and considering protein secretion from non-tumor tissues as confounding factors. Their model was used to predict the earliest time point at which a tumor could be detected based on estimates about growth and excretion rates of tumors. The authors studied CA-125, a Food and Drug Administration-approved biomarker for ovarian cancer, and used the excretion rates and half-life available from the literature. They found that when considering the contribution of healthy cells to the CA-125 concentration in serum tumors could only be detected when they reach tens of millimeters in diameter, which based on known tumor growth rates would be more than 10 years after initiation (6). Although this study provided a framework for the analysis of blood-based protein biomarkers and disease progression, experimental validation is missing, and notably individual variation and the fluctuations of protein excretion over time were not considered in the model.

Mouse models have long been used in cancer research and notably to study breast cancer protein biomarkers (7). Transgenic mice as well as human cancer xenografted into mice have been exploited to uncover circulating cancer-related proteins and tumor cells (8–13). Time course analysis can

From the ‡Biomedical Engineering Department, §McGill University and Genome Quebec Innovation Centre, ‖Rosalind and Morris Goodman Cancer Research Centre, and **Department of Neurology and Neurosurgery, McGill University, Montréal, Quebec H3A 0G1, Canada

⌘ *Author's Choice*—Final version full access.

Received, November 17, 2014, and in revised form, February 11, 2015

Published, MCP Papers in Press, February 13, 2015, DOI 10.1074/mcp.M114.046516

Author contributions: H.L., S.B., P.M.S., and D.J. designed research; H.L., S.B., and M.G.A. performed research; H.L. analyzed data; H.L. and D.J. wrote the paper; D.J. coordinated collaboration.

improve the accuracy of biomarkers and help evaluate the course of cancer progression. One challenge to time course studies in mice is that at most 50–100 μl of blood can be collected weekly without causing harm to the animals that upon processing translates to only 20–40 μl of plasma. This small volume is insufficient for many analytical methods and makes multiplex analysis even more challenging. Previous longitudinal studies either sacrificed individual mice at each time point to extract all the blood at once or pooled the blood extracted from many mice, resulting in the loss of information of individual subjects over time. Recently, a transgenic mouse model was used to characterize the change in plasma proteome at different stages of breast tumor development (14). Plasma samples were collected from tumor-bearing and control mice at three tumor stages and during tumor regression, and the plasma pools from 5–11 mice were measured using mass spectrometry. The plasma proteins that changed in abundance were grouped by their involvement in a number of physiologic processes such as wound repair and immune response, and many of them were found to be tumor microenvironment-derived proteins. However, individual variations could not be studied.

Measuring proteins in blood at concentrations that are relevant for biomarker discovery remains a technological challenge. Arguably the most popular proteomics technology is mass spectrometry; however, it suffers from a bias toward high abundance molecules that mask those of low abundance. The enzyme-linked immunosorbent assay (ELISA) and more specifically sandwich immunoassays constitute the gold standard when it comes to detecting proteins at very low concentrations in samples such as serum or plasma (15). These assay formats have been multiplexed in the form of antibody microarrays and bead-based assays and used to detect proteins in small volumes of blood (16–19). However, multiplexing has a negative impact and can severely compromise assay performance because it increases vulnerability to cross-reactivity among the proteins measured and the mixture of reagents required for these assays, limiting the multiplexed sandwich assays to between 1 and 50 targets depending on the antibodies (20, 21). New assay formats that address this reagent-driven cross-reactivity have been developed (21), and we recently presented an antibody colocalization microarray (ACM)[1] that replicates the performance of single-plex ELISA but is multiplexed and scalable (20). With the ACM, capture antibodies (cAbs) are arrayed on a slide, and each detection antibody (dAb) is spotted on the antigen-cAb spot such that only a single pair of antibodies is used in each microspot, thus avoiding reagent-driven cross-reactivity (21) caused by mixing of the different dAbs. Moreover, we presented a hand-held version of the ACM using a so-called snap chip transferring prespotted and stored antibodies from microarray to microarray, which avoids the spotting procedure during an assay, thus greatly simplifying the operation, that was used to measure 10 proteins simultaneously (22).

In this work, we present a temporal analysis of protein concentration in the serum of individual tumor-bearing mice by measuring 50 proteins using a snap chip ACM. Human MDA-MB-231-1833TR breast cancer cells, which are representative of the triple-negative breast cancer subtype, were injected orthotopically into mice, and blood was collected each week while recording tumor volume. Among the 50 human proteins analyzed, 38 were detected in the serum of tumor-bearing mice, and 10 of these displayed a temporal increase. Protein concentration and tumor size were compared, and the proteins that increased the most during tumor growth were identified. Candidate biomarkers to discriminate between tumor-bearing and healthy mice were validated at each time point after cancer cell injection using ROC curves based either on (i) an absolute threshold or (ii) a self-referred differential methods. The earliest time point at which cancer could be diagnosed was evaluated for both individual proteins and selected protein panels, and the sensitivity and specificity of both methods were compared for different time points of tumor growth.

EXPERIMENTAL PROCEDURES

Materials—Matched antibody pairs for sandwich immunoassays and human antigens used in this study are listed in supplemental Table 1. G-CSF and GM-CSF mouse antigens were purchased from PeproTech, and TNF-RI mouse antigens were from R&D Systems. Streptavidin-conjugated Cy5 was purchased from Rockland. Phosphate-buffered saline (PBS) tablets were obtained from Fisher Scientific. Tween 20 and glycerol were purchased from Sigma-Aldrich. Bovine serum albumin (BSA) was obtained from Jackson ImmunoResearch Laboratories. BSA-free StabilGuard Choice Microarray Stabilizer was purchased from SurModics, Inc. Aminosilane-coated slides were obtained from Schott North America, and nitrocellulose-coated slides were purchased from Grace Bio-Laboratories, Inc. ELISA kits for human G-CSF and human sTNF-RI/TNFRSF1A were purchased from R&D Systems.

Injection of Cancer Cells into Mice and Collection of Mouse Sera—All animal experiments were conducted according to the protocol approved by the McGill University Animal Care Committee. One million MDA-MB-231-1833TR cells (an MDA-MB-231 variant that metastasizes to bone (23)) were injected into the fourth mammary fat pad of SCID/beige mice in 50:50 PBS:Matrigel (BD Biosciences). Blood samples were collected through the saphenous vein 1 week prior to and weekly following the injection of tumors cells. All mice were over 20 g, which allowed us to collect 100 μl of blood per mouse maximum per week, corresponding to 15–40 μl of serum depending on the collection volumes. At the end of the study, the mice were sacrificed, and their blood was collected. Serum was isolated by centrifugation of blood samples in microcuvette tubes (Sarstedt), and the isolated sera were stored at −80 °C for further analysis.

[1] The abbreviations used are: ACM, antibody colocalization microarray; PBST, PBS containing 0.1% Tween 20; dAb, detection antibody; cAb, capture antibody; ROC, receiver operating characteristic; AUC, area under curve; G-CSF, granulocyte colony-stimulating factor; GM-CSF, granulocyte/macrophage colony-stimulating factor; TNF-R, tumor necrosis factor receptor; EGFR, epidermal growth factor receptor; uPA, urokinase-type plasminogen activator; uPAR, urokinase-type plasminogen activator receptor; CEA, carcinoembryonic antigen.

Measurement and Calculation of Tumor Volumes—In this study, we measured the length and width of the tumors at each time point using a caliper and calculated the tumor volume with an ellipsoid model (24).

Preparation of Capture and Detection Antibody Microarrays on Slides—cAb solutions with 20% glycerol and 1% BSA in PBS were spotted on an aminosilane slide with 0.4 nl per spot, snapped with a nitrocellulose slide (assay slide) using the snap apparatus for 1 min, and then separated, and the antibody spots were transferred to the nitrocellulose slide. dAb solutions containing 20% glycerol and 1% BSA in PBS were printed on another aminosilane slide (dAb slide) with 0.8 nl per spot. The concentrations of the cAbs and the dAbs in printing buffers are listed in supplemental Table 1. An inkjet spotter (Nanoplotter 2.0, GeSiM Gesellschaft fuer Silizium-Mikrosysteme mbH) was used for printing at a relative humidity of 80%. The center-to-center distance between spots was 400 μm.

The transfer slides and the assay slides were fixed in two chucks of a snap apparatus and snapped together for antibody transfer. A rubber cushion was used behind each slide, and a spacer was sandwiched between the two slides to ensure reliable reagent transfer (22). After snapping, the assay slide with transferred cAbs was incubated at 4 °C overnight in a sealed chamber and then washed three times with PBS containing 0.1% Tween 20 (PBST) for 5 min each time on the shaker at 450 rpm. Next, the slide was blocked with StabilGuard for 1 h on the shaker at 450 rpm and dried with nitrogen gas.

Storage of the Snap Chip Slides—Both the assay and dAb slides were stored in a −20 °C freezer sealed in an airtight bag with desiccant.

Sandwich Immunoassays with 50 Proteins—Sealed bags of assay slides were removed from the freezer and kept at room temperature for 30 min before opening to avoid condensation. To make standard curves, 50 proteins were spiked in PBS containing 0.05% Tween 20 at the concentrations listed in supplemental Table 1, and 5-fold, seven-point dilution series were prepared. A buffer solution without any proteins was also prepared as a blank control. All mouse serum samples were diluted five times using PBS containing 0.05% Tween 20. GFP was used in each array for data normalization. The assay slides were clamped with 16-compartment slide module gaskets (Grace Bio-Laboratories, Inc.), and then 75–80 μl of each serially diluted standard protein solutions and diluted mouse serum samples were incubated on the assay slides on the shaker at 450 rpm at 4 °C overnight. The slides were then rinsed three times with PBST on the shaker at 450 rpm for 5 min each time followed by a brief rinse with distilled water and dried with nitrogen gas. The sealed bags of dAb slides were removed from the freezer and kept at room temperature for 30 min, then the bags were opened, and the dAb slides were incubated in a humidity-saturated Petri dish for 20 min to rehydrate glycerol droplets containing antibodies. Next, the assay and the dAb slides were fixed in the snap apparatus and snapped together for 1 min. Following separation, the assay slides were incubated in a humidified Petri dish for 1 h, then clamped with the gasket, and rinsed four times with PBST on the shaker at 450 rpm for 5 min. The assay slides were then incubated with 2.5 μg/ml streptavidin-conjugated Cy 5 for 20 min on the shaker at 450 rpm, then rinsed three times with PBST on the shaker and once with distilled water, and dried using nitrogen gas.

Scanning of the Slides and Data Analysis—The slides were scanned using a microarray laser scanner (Axon GenePix 4000B) with the 635 nm laser. The net fluorescence intensity of a spot was extracted using Array-Pro Analyzer version 4.5 (Media Cybernetics) by subtracting the background signal in the vicinity of each spot.

Heat maps were produced using the Spearman's rank correlation coefficient between the protein levels. For each of the seven time points, the rank was computed for each protein, and the absolute difference between each Spearman coefficient was used to determine the similarity matrix for hierarchical clustering analysis. The Z-score represents the distance between a data point and the mean in units of the standard deviation.

For all top ranked 10 proteins, the concentrations for all 14 mice at seven time points were normalized between 0 and 1 using the following formula: $(x - \min(x))/(\max(x) - \min(x))$. In the absolute threshold method, the disease cohort consisted of the 11 tumor-bearing mice and the blood concentration of the proteins at that specific time point. The control values for each time point consisted of the concentration of proteins from three control mice at seven time points, adding up to 21 "controls." This control cohort was used both for ROC calculation and for calculating the sensitivity and specificity described further below. In the differential method, for each disease and each control mouse, the (normalized) average concentration from weeks −1 and 0 were subtracted from the concentration at each time point. For ROC curve calculation, the control cohort comprised the concentration value for each of the three control mice; there were thus three controls for each of the five specific time points. ROC curves were calculated and plotted using GraphPad Prism 6 (GraphPad Software).

For the time course analysis, the sensitivity and specificity of individual proteins and a protein panel were calculated for both the absolute threshold and differential method for each week. The six proteins whose area under curve (AUC) values are highest in week 3 using either absolute or differential methods were selected for time course analysis. For the absolute threshold method, the threshold for a positive diagnostic was defined as a measurement higher than the average plus two standard deviations of the 21 controls. For the differential self-referenced method, the threshold for a positive diagnostic was defined as a concentration above the average of weeks −1 and 0 (for the same mice) plus 2 times the average of the standard deviations that were calculated from the seven time points for the three control mice. For a protein panel, the same aforementioned calculation method was applied to each protein first, and then either the averaged threshold or averaged baseline was used. Sensitivity was defined as the true positive rate, and specificity was defined as the true negative rate.

RESULTS

Fabrication of Antibody Microarrays—The procedure for making antibody microarrays and performing the multiplex immunoassay in an ACM format with a snap chip (22) is illustrated in Fig. 1. In ACMs, each dAb is delivered only to the corresponding cAb spot, thus avoiding cross-reactivity and false positive signals. Whereas previously only one snap and transfer were performed (22), we implemented a novel "double transfer" protocol that we recently developed to improve the alignment between cAb and dAb microarrays.[2] Briefly, whereas previously only the dAbs were transferred to the assay slide by snapping, here both cAb and dAb microarrays are transferred to minimize misalignment and thus increase the density of spots that may be transferred (Fig. 1). We established a snap chip targeting 50 human proteins (supplemental Table 1) comprising cancer biomarkers, cancer-related proteins, and cytokines. For all assays, standard curves were established for each target protein.

Validation of the Snap Chip Immunoassay—To assess whether the assays effectively discriminate between the hu-

[2] H. Li, J. D. Munzar, A. Ng, and D. Juncker, submitted manuscript.

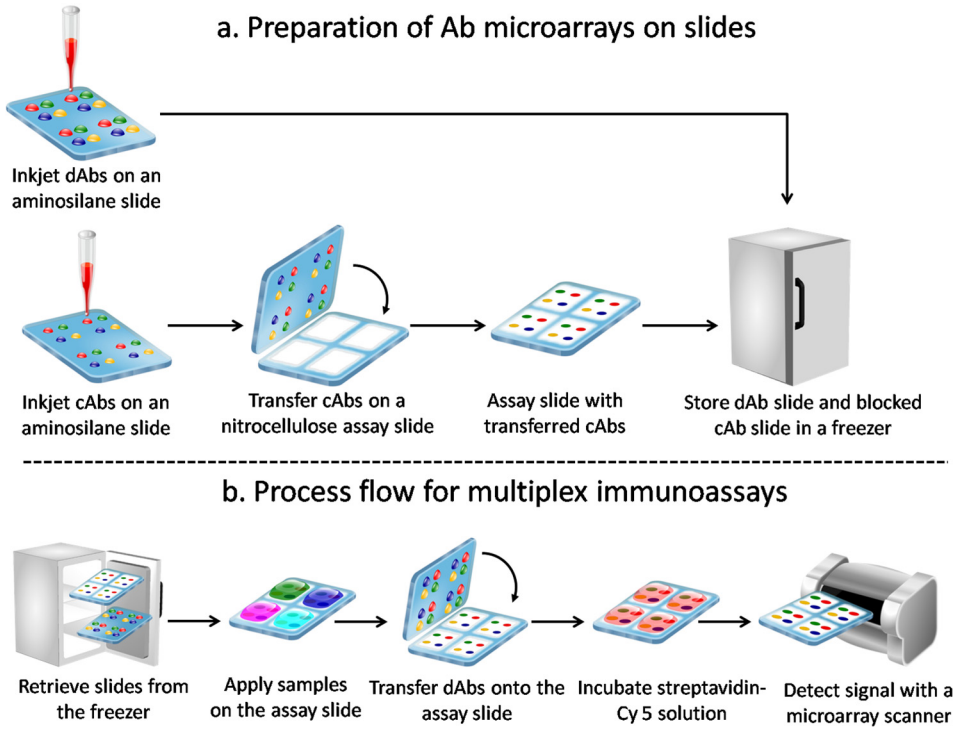

FIG. 1. **Schematic outlining the process flow for preparing the slides and performing an antibody colocalization microarray in a snap chip format.** *a*, dAbs are spotted onto an aminosilane-coated slide that is stored in a freezer. cAbs are spotted onto another aminosilane-coated slide with the same spotting layout and transferred to a nitrocellulose-coated assay slide followed by blocking and storage in a freezer. *b*, both slides are removed from the freezer prior to use. The assay slide is incubated with sample solutions, and then the dAbs are transferred to the assay slide by snapping followed by incubation with streptavidin-Cy 5. Next, the assay results are imaged with a fluorescence microarray scanner, and the data are analyzed.

man proteins secreted by the xenograft tumor from mouse proteins, the interspecies cross-reactivity was assessed. Cross-reactivity to mouse proteins was not expected as the antibody pairs we used were produced in mice (25), but we nonetheless tested it experimentally for three recombinant mouse proteins, G-CSF, GM-CSF, and TNF-RI. Binding of mouse proteins was undetectable up to the maximal assay concentration of 400 ng/ml, indicating that the antibodies are indeed specific for human proteins.

Next, we compared the snap chip immunoassay with a commercial ELISA for G-CSF and TNF-RI. These two proteins were measured in 16 mouse serum samples comprising 14 sera collected at the end of the study and two samples of mixed mouse serum samples from earlier time points (for more details, see below). Duplicate measurements of each sample were made for both snap chip and ELISA (supplemental Fig. 1). The correlation, *r*, for G-CSF and TNF-RI proteins was 0.94 and 0.82, respectively. The slope of the curve for G-CSF was 0.97, whereas it was 1.5 for TNF-RI. Such differences are commonly observed for immunoassays (26, 27). This discrepancy might be due to different antibody clones used in the two methods, although they were purchased from the same vendor, or the use of different buffers imposed by the use of the snap chip and of a mixture of the proteins for the dilution series. We do not expect this difference to affect the results of the time course measurements as relative changes are assessed.

Serum Protein Levels Measured during the Growth of Primary Mammary Tumor Xenografts in Mice—Human triple-negative breast cancer cells (MDA-MB-231-1833TR) were injected into the mammary pad of 11 mice, and Matrigel devoid of breast cancer cells was injected into three control mice. Tumors grew in all 11 mice and were measured weekly starting at week 2, the first time point at which they were palpable. Initial blood samples were collected 1 week and ~1 h before cell injection, and then on a weekly basis starting on the 2nd week. In total, seven samples were collected from each mouse, adding up to 98 samples in total. The concentrations of the 50 proteins in each sample were measured with the snap chip, which could accommodate up to 16 samples per chip (slide), whereas on some chips, one column of 8 wells was used for establishing the binding curve. Among 50 proteins measured with ACM, the levels of 38 proteins were above the limits of detection of the assay for at least one time point and thus considered measurable in mouse sera. The remaining 12 proteins were not detected in the serum.

A hierarchical clustering was performed for 38 human proteins based on the average concentration across the 11 mice at each time point (Fig. 2). Ten proteins, clustered from EGFR down to MMP-3, show increasing concentrations over time.

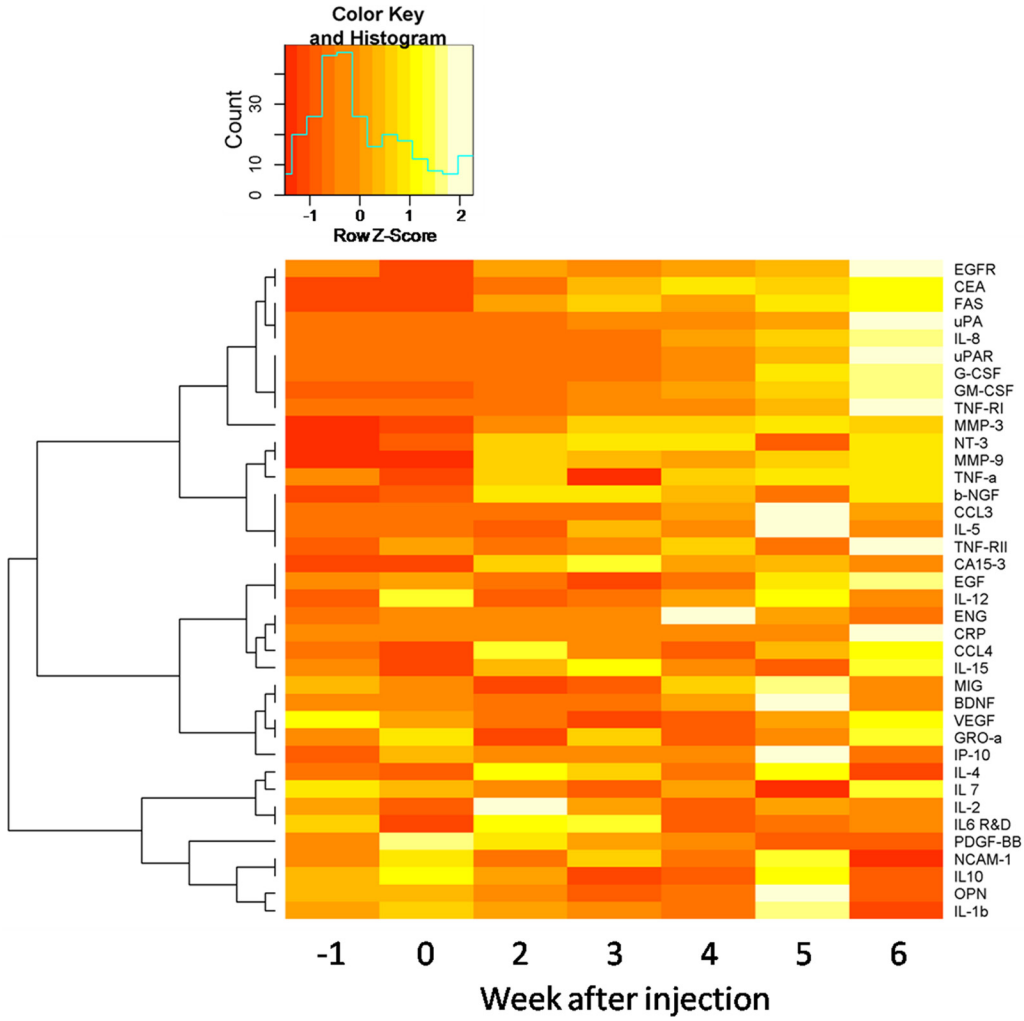

FIG. 2. **Hierarchical cluster analysis of the 38 human proteins detected in mouse sera.** The average concentration of each protein of the 11 tumor-bearing mice subtracted by the average concentration of three control mice is shown. Row Z-scores were used for color rendering.

The next cluster of seven proteins from NT-3 to TNF-RII also shows a clear increase of average values over time but with significant fluctuation. Further down in the list, no clear trends are visible. The proteins clustered at the bottom, starting from IL-4, show moderate signals at week −1 and low signal levels for time point 6, and some of them are relatively high for time point 5. HER2 was not detected in the mouse serum as expected because triple-negative breast cancer cells were used to grow tumors. CA 15-3, which is used clinically to evaluate response to therapy in breast cancer (28), did not cluster with the discriminating proteins at the top. CA15-3 did, however, increase in concentration during the first 3 weeks after cancer cell injection but then decreased, and fluctuations were observed in individual mice. For further analysis, we decided to focus on the 10 proteins clustered at the top of the heat map.

The time course of tumor growth is shown in Fig. 3, *top left panel*. The results show important variations from animal to animal. Although variability in tumor growth is generally known, it should be noted that all cancers originated from a cell line with reduced genetic variability compared with natural tumors and were implanted in mice with similar genetic background, and yet widely varying growth rates and final tumor volumes are observed despite the homogeneous genetic background. To further investigate the 10 increased proteins found in Fig. 2, we plotted their concentrations during tumor growth for both individual mice and the average of all tumor-bearing and control mice. Six proteins (G-CSF, IL-8, TNF-RI, uPA, uPAR, and GM-CSF) increased continuously during the growth of human xenografts with only small fluctuations, and the remaining four proteins (EGFR, CEA, MMP-3, and FAS) also increased but with significant fluctuation (Fig. 3). EGFR shows relatively high signals in control mice, which might be due to the cross-reactivity of antibodies with other antigens (20). Regardless, on average, a clear trend is visible for EGFR as the signal rises significantly. The fluctuation in protein concentrations in samples taken prior to cancer cell injection (week −1 and week 0) and of control animals might be as-

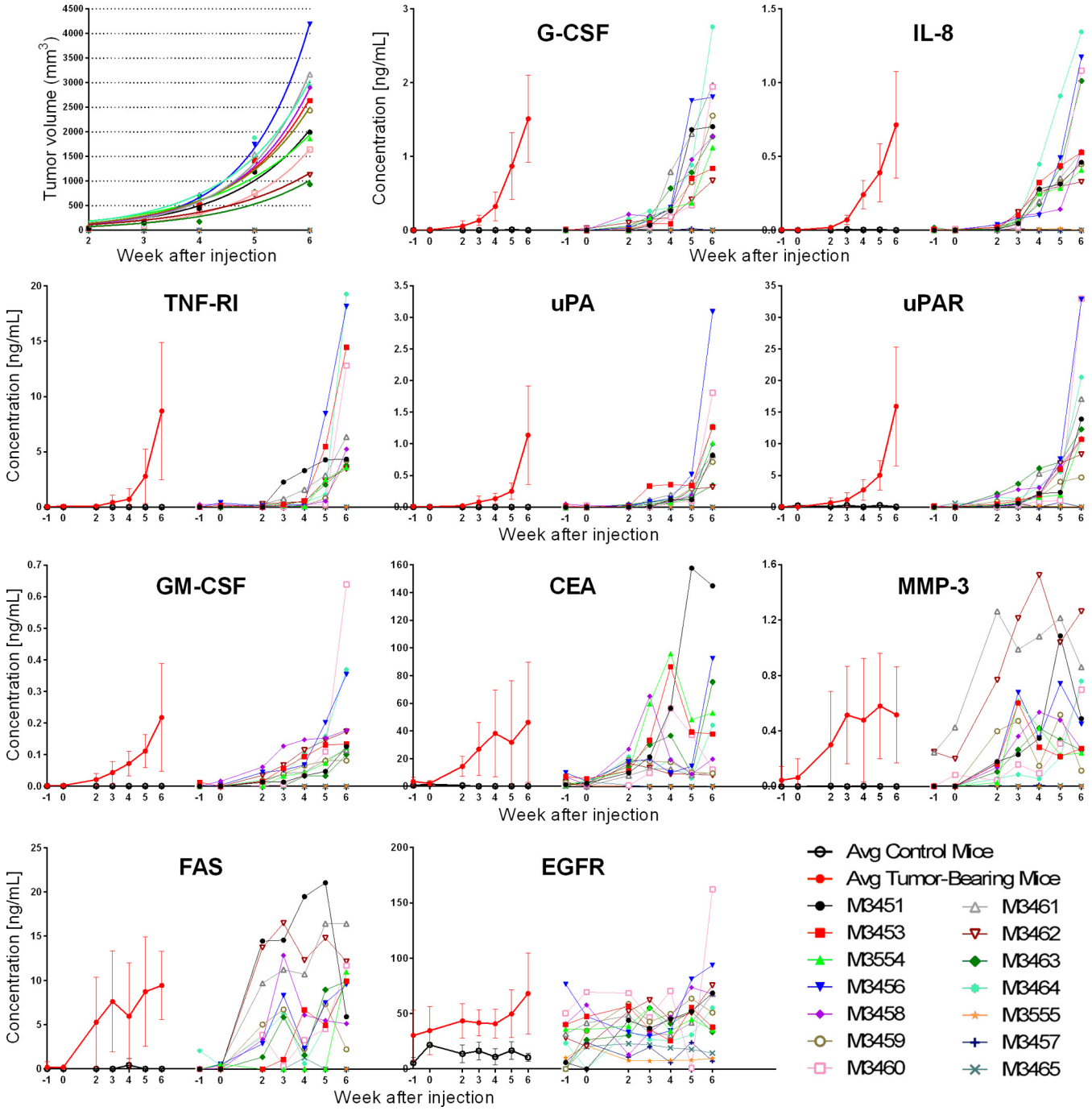

FIG. 3. **Tumor volumes and protein concentrations during the time course of tumor growth.** *Top left panel*, tumor volume of the 14 mice (comprising three controls) calculated for weeks after the injection of cancer cells and fitted with an exponential growth curve. The remaining panels show the time course of the 10 proteins (G-CSF, IL-8, TNF-RI, uPA, uPAR, GM-CSF, CEA, MMP-3, FAS, and EGFR) that increased during the growth of the human breast cancer xenografts in mice. For each protein, curves on the *left* show average (*Avg*) protein levels for the tumor-bearing mice and controls during the growth of tumor, and curves on the *right* show protein levels during the time course for each of the 11 individual tumor-bearing mice and three controls. *Error bars* on the average curves are the standard deviations of protein concentrations among mice. M3451–M3465 represent the identity of each mouse.

cribed to the variability in sample collection and serum and the specificity of the antibodies. The correlation between tumor size and protein concentration was not consistent among mice. Mice M3456 and M3464 grew large tumors, and the concentration of proteins in blood was also high in relation to the other mice. However, M3460 shows a moderately sized tumor but high concentrations of proteins in the blood, indicating that the correlation between protein concentration and

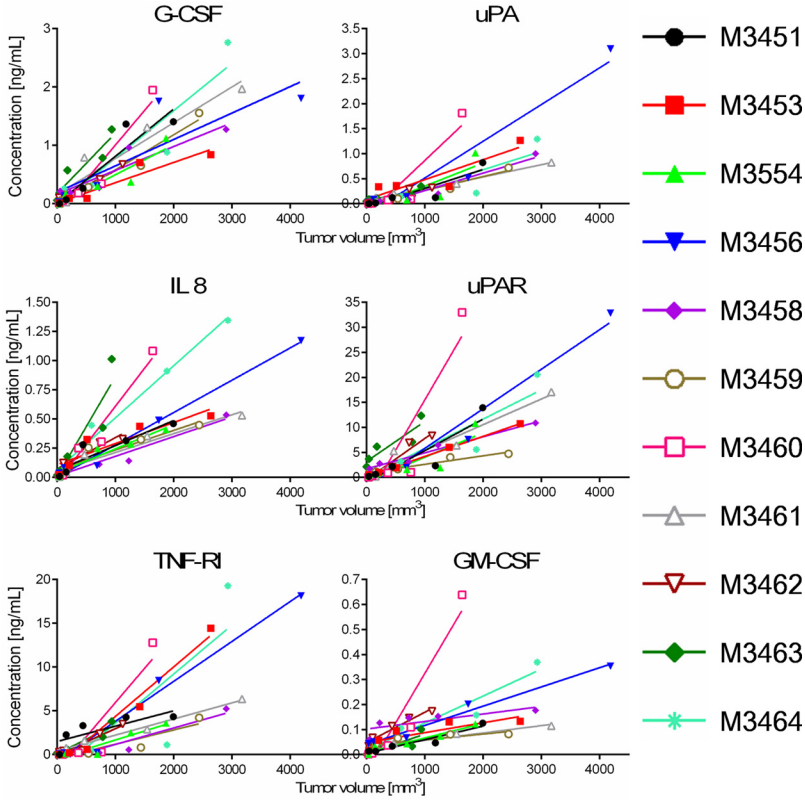

FIG. 4. **Comparison between tumor volume and protein concentration of the six proteins G-CSF, IL-8, TNF-RI, uPA, uPAR, and GM-CSF in serum for each of the 11 mice along with linear regression curves.** Despite the genetic homogeneity of the mice, important variations are seen among mice. A high or low excretion rate for one protein is often mirrored by the excretion rate for other proteins, suggesting that metabolic differences between tumors underlie this variation.

tumor size is not consistent among different mice as will be further discussed below.

Correlation of Protein Levels with Tumor Volumes—With mice, it becomes possible to track the time course of tumor size and protein concentration in blood for an extended period of time, allowing one to directly probe a model linking the two. We plotted the six proteins whose levels increased continuously along with the growth of the tumor burdens for each of the 11 tumor-bearing mice (Fig. 4). We found that the protein levels and the tumor volumes were linearly correlated for all mice (supplemental Table 2).

Time Course Analysis of Sensitivity and Specificity of Protein Biomarkers—For the diagnosis and monitoring of recurrence, the differential change in concentration (sometimes also called the velocity (1)) is often more accurate. Indeed, this measure intrinsically takes into account personal variation and defines individual baselines. Here, we wanted to test whether differential, self-referred diagnosis would outperform diagnosis relying on a population average-based threshold in mouse cancer models. The ROC curves of the 10 individual proteins as well as of the linear combination of the normalized variation of the 10 proteins for each time point are plotted. The ROC curves calculated using absolute and differential methods for the six proteins that linearly correlated with tumor burden are shown in Figs. 5 and 6. The ROC curves for the four proteins that increased but fluctuated are shown in supplemental Figs. 2 and 3. The AUC shows that diagnostic accuracy for all the proteins increased progressively during the time course of tumor growth as might be expected for these mouse models. The low AUC values for mouse from weeks 0 and −1 using the absolute threshold method indicate that the results reflects a change in the mouse except for TNF-RI where already a high AUC values arises before; this may be due to a measurement artifact or a coincidental higher expression in the specific subset of mice. For most proteins, the differential method and the absolute threshold analysis yielded a similar diagnostic accuracy. Using the differential method, IL-8 achieved the best performance of AUC = 1 for all the time points after injection of cancer cells, which is also reflected in its time course curves for each individual mouse shown in Fig. 3. Interestingly, the AUC already reaches a high value after only 2 weeks. For example, in week 2, MMP-3 and IL-8 show an AUC = 1 with absolute and differential methods, respectively (supplemental Figs. 2 and 3).

The ROC curve of the 10-protein panel was outperformed by individual proteins that yielded higher AUCs. A backward elimination protocol (29, 30) was used to identify panels with higher sensitivity and specificity for both differential method and threshold analysis. Following the removal of each individual protein from the panel, the sum of sensitivity and specificity was calculated, and only the panels with better or equivalent accuracy were selected for further elimination. Using this procedure, we found 37 combinations with between eight and four proteins with sensitivity = 1 and specificity = 1 for every time point as listed in supplemental Table 4. CEA, FAS, and uPAR appeared in all 37 combinations. To further select the

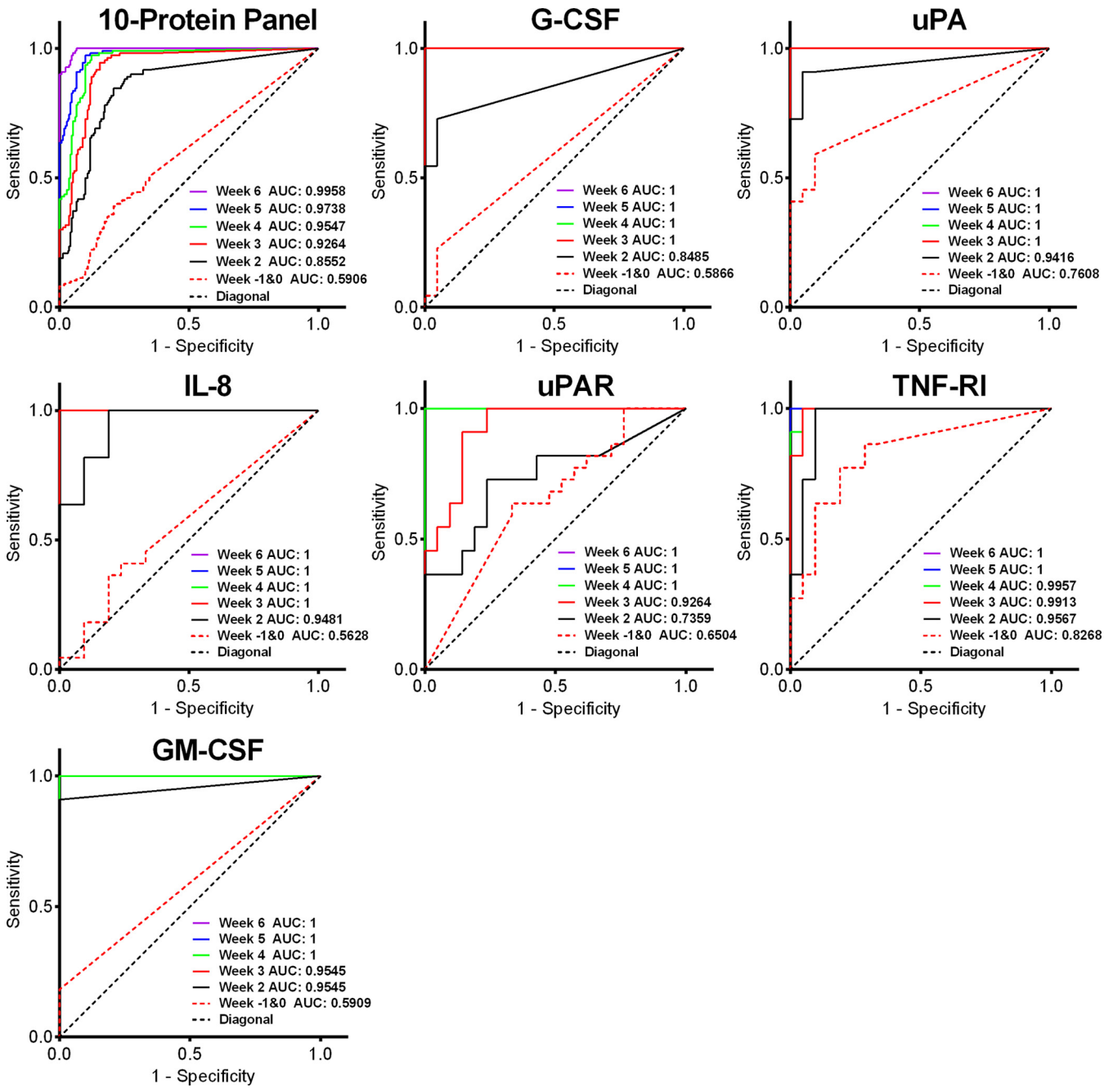

FIG. 5. **ROC curves of the 10-protein panel and six individual human proteins at each time point before and after injection of cancer cells using the absolute threshold method.** For overlapping curves for AUC = 1, the color from the earliest week at this value is shown.

best combinations and taking advantage of the control time points at weeks −1 and 0, we calculated the diagnostic specificity using the absolute threshold-based method and found eight combinations with a specificity of 0.96.

The sensitivity and specificity were computed for six individual proteins whose AUC = 1 at week 3 using either the absolute or differential method. The optimal protein panel comprising CEA, FAS, uPAR, and IL-8 was computed using an absolute threshold of two standard deviations above the average of the control mice or using the differential method with a limit set as the average standard deviation above the value at weeks −1 and 0 (see "Experimental Procedures" for details). The sensitivity and specificity for each time point are shown in Fig. 7. At week 2, the sensitivities of G-CSF and IL-8 were higher for the differential threshold, and those of uPA, MMP-3, and EGFR were higher for the absolute threshold. The sensitivity improved monotonically for most individual proteins. Relatively large fluctuations are observed for the specificity that can be accounted for by the small number of control mice. CEA gives the most accurate classification with

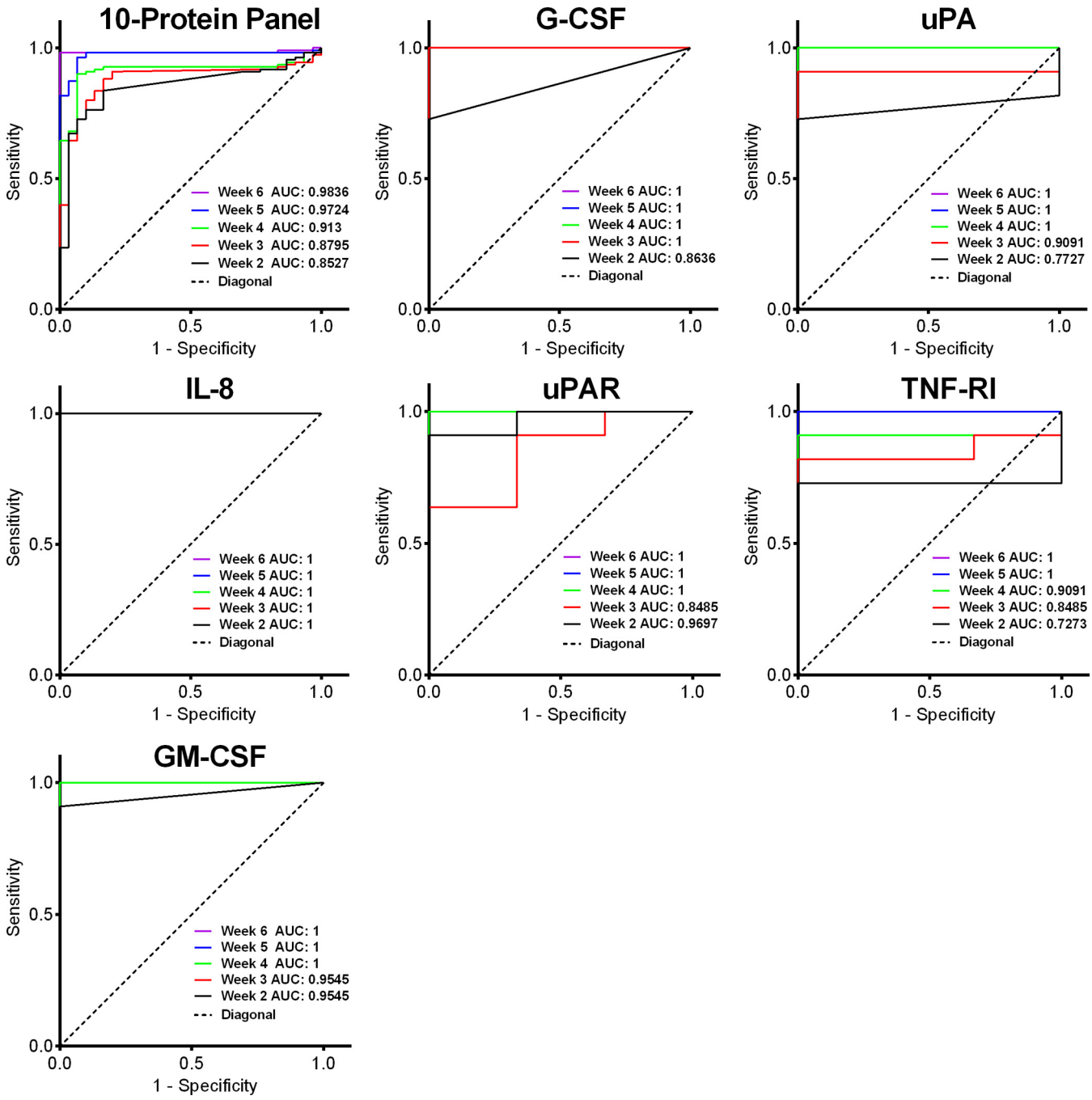

FIG. 6. **ROC curves of the 10-protein panel and six individual proteins at each time point after cancer cell injection using the self-referenced differential method.** Some curves with AUC = 1 are invisible due to overlap with other curves. Unlike for the absolute threshold, no ROC curves were plotted for weeks −1 and 0 because they are not meaningful.

both measurements between weeks 2 and 6 because the assay signals in tumor-bearing mice are higher than those in the control mice. The specificity is similar for both methods except for IL-8 and uPA. EGFR showed a relatively low sensitivity using the differential method that can be ascribed to the fluctuations in concentration observed in our measurements. Despite the fluctuations observed, our measurements achieved relatively high sensitivity and specificity starting from as early as the 2nd week depending on the proteins in question.

DISCUSSION

In this study, we detected 38 human proteins in mouse serum, and the 10 selected proteins found to increase over time in the sera of tumor-bearing mice had previously been linked to triple-negative breast cancer, consistent with the

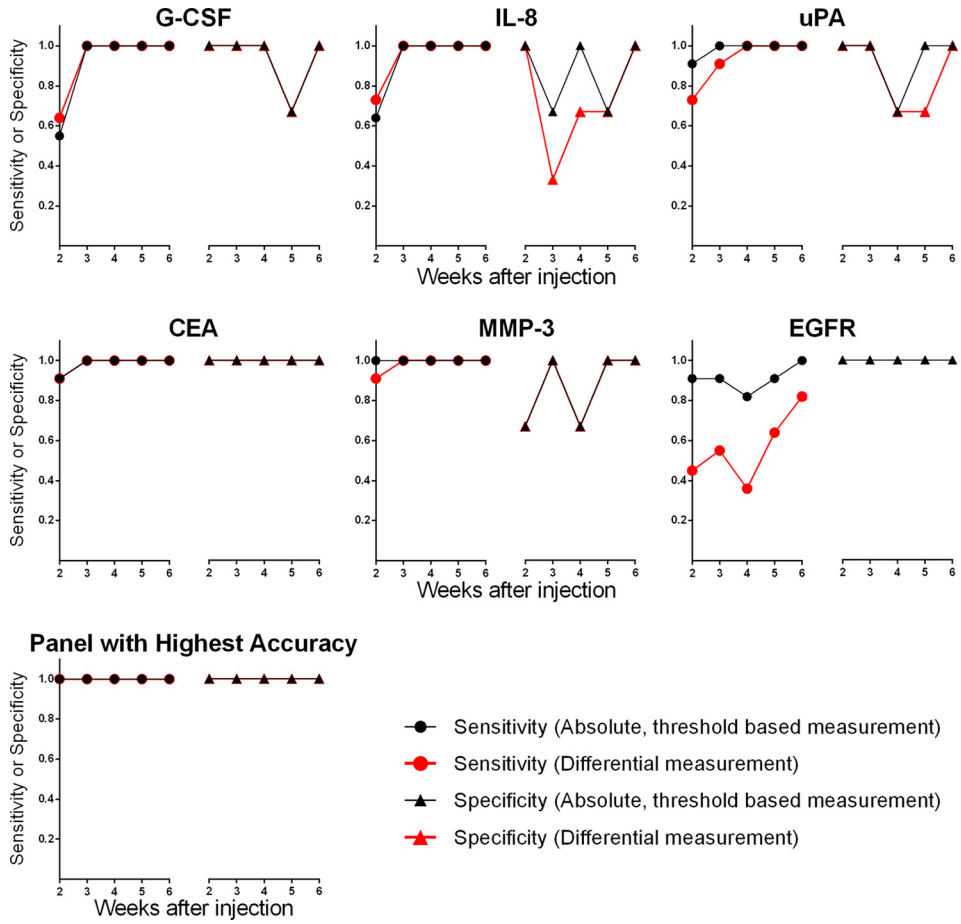

FIG. 7. **Time course of sensitivity and specificity calculated with the absolute threshold-based method and differential measurement for the six proteins whose AUC = 1 at week 3 as well as the panels with sensitivity = 1 and specificity = 1.**

cancer subtype of MDA-MB-231 cells. G-CSF has been reported to be a support drug in chemotherapy of triple-negative breast cancer (31). Higher concentrations of IL-8 were found to be correlated with the invasion and metastasis process for MDA-MB-231 cells (32–34). TNF-RI is associated with poor prognosis in breast cancer patients on its own (35). The uPA/uPAR system is involved in multiple steps of tumor formation and progression (36, 37), and the uPA/uPAR genes were found to be overexpressed in MDA-MB-231 cell lines (38). GM-CSF is a cytokine functioning in tumor progression and has been found to be overexpressed in MDA-MB-231 and other breast cancer cells (39). CEA was found in the blood of triple-negative breast cancer patients and was documented in the majority of patients with metastatic breast cancer (40). EGFR is a cell surface receptor that has been found to be expressed in many human tumor cells including MDA-MB-231 cells; it contributes to cancer cell proliferation and migration (41–43) and can function as a potential therapeutic target in triple-negative breast cancer (44). MMP-3 is involved in tumor invasion and metastasis and has been reported to be highly overexpressed in MDA-MB-231 cells (45). FAS was found to mediate non-apoptotic functions in triple-negative breast cancer cells (46, 47). These previous studies indicate that these proteins function in different aspects of triple-negative breast cancer and therefore are concordant with a higher concentration in blood as the tumor grows.

In a previous study using a HER2/neu-driven inducible endogenous cancer mouse model, 36 candidate protein biomarkers were found to be increased in the mouse plasma using mass spectrometry (8). The proteins identified were distinct from those identified in this study; however, in consideration that the cell line used here represents a triple-negative cancer, it is expected that different markers would be found. Some of the proteins were detected at the pg/ml range in this work, lower than ng/ml concentrations for most of the 36 proteins detected using mass spectrometry in the previous work.

Considering that we are only measuring human proteins, which are not expected in the blood prior to starting the experiment, one would not expect to obtain a detectable signal prior to tumor cell inoculation, but a number of proteins show weak to moderate signals in week −1 and week 0 (Fig. 2). Cross-reactivity to mouse proteins is possible for the antibodies, which are not of murine origin, but unlikely for most

proteins given that most capture antibodies are mouse antibodies (see supplemental Table 1). The variability observed may in part arise from the difference in matrix between the binding curves made in buffer and the actual measurements that were conducted in serum, which is known to generate a background signal. Hence some signals that appear above the limit of detection may in fact be below. This issue is a general challenge faced by all sandwich assays such as ELISA due to the absence of a reference sample.

Gambhir and co-workers (5, 6) proposed mathematical models relating protein levels with tumor volumes and predicted that with the limits of detection of current ELISA tumors could not be detected until they reach tens of millimeters in diameter. Despite the relatively large size of tumors, the concentration of proteins was only in the pg/ml range (Fig. 3), which is close to the limit of detection of ELISA and the snap chip ACM and similar in concentration to those found in humans. Considering that the volume of blood in a mouse is ~2500 times less than that in a human (48), the relatively low concentration of cancer proteins in the blood of mice can be ascribed to a number of factors. This xenograft model elicits much less vascularization than many natural tumors and rapidly develops a necrotic core within the tumor. In addition, differences in protein shedding and vascular permeability as well as different half-lives of the proteins in blood could all contribute to reduce the concentration of tumor proteins in blood (6). Moreover, proteins from stromal cells surrounding the tumor, which are also altered, are expected to be released into the blood and to contribute to the increase in concentration (14, 49). However, because the antibodies used here are specific for human proteins, stromally released proteins could not be measured here. Indeed, the protein concentrations measured in this work are lower than those in a previous study using an inducible endogenous HER 2/neu mouse model that measured proteins at high ng/ml range (14), suggesting that the xenograft cancer model might yield lower protein concentrations in blood.

We found that protein concentration was proportional to tumor size in agreement with the model proposed by Lutz *et al.* (5) (Fig. 4). However, the necrotic core of these xenograft tumors that arises for volumes as small as 300–500 mm^3 (~8 mm in diameter) might break the direct relation between tumor volume and cell numbers. Cells are mainly proliferating within a viable rim at the edges of the tumor, and hence one would expect that the contribution to proteins in the blood would originate from those cells. This would imply that biomarker concentration would be correlated to tumor surface area. When comparing the protein concentration with the surface area of the ellipsoid tumor, a linear regression provides the best fit with comparable accuracy relative to volumetric fits (supplemental Tables 2 and 3). The tumor outer layer is in fact heterogeneous, and hence secretion may occur both from the outer surface and from within the tumor, providing a plausible explanation for the results observed. Extending the growth time toward larger tumors might help resolve this question; however, the tumor sizes reached the maximal allowable tumor volumes under the approved animal use protocol.

Some of the most important findings of this study are (i) the significant fluctuations in the relations linking the protein concentration and tumor volume and (ii) the variability in the excretion rates among different mice. As illustrated in Fig. 4, for many proteins and many mice, the data points are not aligned with the linear fit and fluctuate above and below the fit. These results indicate that the relationship between excretion rate and blood concentration is not constant and may vary because of environmental factors and metabolic activity. Additionally, the range of slopes for protein concentration *versus* tumor volumes varies significantly. M3459 is typically characterized with the lowest slopes, whereas M3460 has the highest slopes. The highest and lowest ratios between protein excretion rate normalized for tumor volume for the six proteins measured were found for IL-8 and TNFR-I. For IL-8, the slope of M3460 is 6.5×10^{-4}, and that of M3459 is 1.7×10^{-4}, corresponding to a ratio of 3.8, and for TNFR-I, the slope for M3460 is 7.8×10^{-3}, and that for M3459 is 1.6×10^{-3}, corresponding to a ratio of 4.9. These results indicate that in addition to different excretion rates as a function of tumor volume even larger fluctuations in protein secretion rates arise between mice with highly similar genetic background and that they can arise independently of tumor growth rates. The variability in protein concentration will add uncertainty in the size of the tumor that may be detected and might prevent the establishment of precise concentration cutoffs for cancer diagnosis considering large personal variations among human patients at least when using single protein biomarkers. Indeed, studies of breast cancer growth in human patients monitored by mammography screening have shown large variations between patients (50). Interestingly, the excretion rates of different proteins are conserved relative to other mice; *i.e.* a mouse that had a high concentration of one protein in blood also had a high concentration of the other five proteins that were studied here. This may reflect the metabolic activity of a single tumor that leads to a consistent excretion rate for different proteins. If the same relationships hold true in human tumors, one protein could be used for normalization of the values.

As shown from the ROC curves, the blood-based classification identified tumor-bearing mice after only 2 weeks when many tumors were not yet palpable (Figs. 5 and 6). The AUC values for most of the 10 individual proteins outperform the multiprotein panel diagnostic. The panel is simply the collection of all proteins, and hence it would be expected that some individual proteins outperform it. Finally, we evaluated the sensitivity and specificity of individual proteins for specific thresholds determined based on the standard deviation of the measurement (Fig. 7). Among the six proteins with the highest sensitivity and specificity, three overlapped with the ones that

continuously increased during tumor growth (G-CSF, IL-8, and uPA) whose ROC curves are shown in Figs. 5 and 6, whereas three were distinct (CEA, MMP-3, and EGFR). Following backward elimination, optimal protein panels with higher specificity and sensitivity were identified for both the absolute threshold and differential methods (supplemental Table 4). Interestingly, three of these eight combinations consisted of only four proteins comprising CEA, FAS, uPAR, and either IL-8, TNF-RI, or G-CSF. FAS was neither among the six top proteins for AUC or the sensitivity/specificity analysis but was essential to the high performance of the protein panel. The other five combinations comprised five proteins, and the panels were either a combination of the above proteins or one panel included uPA and another included GM-CSF.

The use of each time point as a negative control afforded a sufficient number of negative controls, but for future biomarker studies, it is recommended to increase the number of negative controls to achieve more robust statistics. This study found little differences between absolute threshold and differential measurements. There are several factors that may contribute to the high accuracy of both approaches, namely the genetic similarity of mice and of the injected cancer cells, the selectivity of our analysis for xenograft proteins, and the limited number of control mice. Future studies may overcome some of the limitations of our study and use both larger cohorts of control mice and validation cohorts (8) as well as more advanced statistical analysis (51, 52). Finally, measuring protein levels using high sensitivity antibody microarrays from induced or spontaneous mouse cancer might uncover other facets of protein concentration in blood that are not replicated by xenograft tumors.

In summary, we measured 50 proteins in serial serum samples from a human xenograft breast tumor model and found 10 proteins that increased in concentration as the tumors grew. For six of these, concentration and tumor volume were linearly correlated. To the best of our knowledge, this is the first study to monitor protein levels at multiple time points in multiple individual xenograft-bearing mice. It will be interesting to evaluate whether these proteins will also be found in the blood of human triple-negative cancer patients. To evaluate proteins secreted from the tumor microenvironment, samples could be measured in parallel with antibody arrays targeting mouse proteins (14). Such time course studies might be repeated with genetically induced cancers in mice and thus study a protein excretion time course in vascularized tumors but also include contributions of the stromal tissue. ROC curves showed that the diagnostic accuracy with identified proteins increased progressively during the time course of tumor growth for both absolute threshold and differential methods. For most individual proteins and the protein panel, the differential measurement showed similar sensitivity and specificity as the absolute threshold-based measurement. Optimal protein panels were selected and outperformed individual proteins. It will be interesting to see whether the same trends will persist with larger cohorts and in other cancer models. Time course studies within an early diagnosis paradigm are logistically difficult for human cancer, but it may be possible to use antibody colocalization microarrays to study the response to therapy in both neoadjuvant and adjuvant settings by serially collecting blood and monitoring the concentration of multiple proteins (53).

Acknowledgments—We thank Professor Rob Sladek for the use of the inkjet spotter and the Center for Structural and Functional Genomics at Concordia University for the use of the fluorescent microarray scanner.

* This work was supported in part by the Canadian Institutes for Health Research, the Natural Science and Engineering Research Council of Canada (NSERC), the Canadian Cancer Society, and the Canada Foundation for Innovation.

S This article contains supplemental Figs. 1–3 and Tables 1–4.

¶ Supported by a fellowship from the NSERC-Collaborative Research and Training Experience (CREATE) Integrated Sensor Systems program.

‡‡ A Canada Research Chair. To whom correspondence should be addressed. E-mail: david.juncker@mcgill.ca.

REFERENCES

1. Nielsen, V. G., and Garza, J. I. (2014) Comparison of the effects of CORM-2, CORM-3 and CORM-A1 on coagulation in human plasma. *Blood Coagul. Fibrinolysis* **25,** 801–805
2. Wang, Q., Chaerkady, R., Wu, J., Hwang, H. J., Papadopoulos, N., Kopelovich, L., Maitra, A., Matthaei, H., Eshleman, J. R., Hruban, R. H., Kinzler, K. W., Pandey, A., and Vogelstein, B. (2011) Mutant proteins as cancer-specific biomarkers. *Proc. Natl. Acad. Sci. U.S.A.* **108,** 2444–2449
3. Joshi, S., Tiwari, A. K., Mondal, B., and Sharma, A. (2011) Oncoproteomics. *Clin. Chim. Acta* **412,** 217–226
4. Füzéry, A. K., Levin, J., Chan, M. M., and Chan, D. W. (2013) Translation of proteomic biomarkers into FDA approved cancer diagnostics: issues and challenges. *Clin. Proteomics* **10,** 13
5. Lutz, A. M., Willmann, J. K., Cochran, F. V., Ray, P., and Gambhir, S. S. (2008) Cancer screening: a mathematical model relating secreted blood biomarker levels to tumor sizes. *PLoS Med.* **5,** e170
6. Hori, S. S., and Gambhir, S. S. (2011) Mathematical model identifies blood biomarker-based early cancer detection strategies and limitations. *Sci. Transl. Med.* **3,** 109ra116
7. Kelly-Spratt, K. S., Kasarda, A. E., Igra, M., and Kemp, C. J. (2008) A mouse model repository for cancer biomarker discovery. *J. Proteome Res.* **7,** 3613–3618
8. Whiteaker, J. R., Lin, C., Kennedy, J., Hou, L., Trute, M., Sokal, I., Yan, P., Schoenherr, R. M., Zhao, L., Voytovich, U. J., Kelly-Spratt, K. S., Krasnoselsky, A., Gafken, P. R., Hogan, J. M., Jones, L. A., Wang, P., Amon, L., Chodosh, L. A., Nelson, P. S., McIntosh, M. W., Kemp, C. J., and Paulovich, A. G. (2011) A targeted proteomics-based pipeline for verification of biomarkers in plasma. *Nat. Biotechnol.* **29,** 625–634
9. Hung, K. E., Faca, V., Song, K., Sarracino, D. A., Richard, L. G., Krastins, B., Forrester, S., Porter, A., Kunin, A., Mahmood, U., Haab, B. B., Hanash, S. M., and Kucherlapati, R. (2009) Comprehensive proteome analysis of an Apc mouse model uncovers proteins associated with intestinal tumorigenesis. *Cancer Prev. Res.* **2,** 224–233
10. Whiteaker, J. R., Zhang, H., Zhao, L., Wang, P., Kelly-Spratt, K. S., Ivey, R. G., Piening, B. D., Feng, L.-C., Kasarda, E., Gurley, K. E., Eng, J. K., Chodosh, L. A., Kemp, C. J., McIntosh, M. W., and Paulovich, A. G. (2007) Integrated pipeline for mass spectrometry-based discovery and confirmation of biomarkers demonstrated in a mouse model of breast cancer. *J. Proteome Res.* **6,** 3962–3975
11. Pitteri, S. J., Faca, V. M., Kelly-Spratt, K. S., Kasarda, A. E., Wang, H., Zhang, Q., Newcomb, L., Krasnoselsky, A., Paczesny, S., Choi, G., Fitzgibbon, M., McIntosh, M. W., Kemp, C. J., and Hanash, S. M. (2008) Plasma proteome profiling of a mouse model of breast cancer identifies

a set of up-Regulated proteins in common with human breast cancer cells. *J. Proteome Res.* **7,** 1481–1489
12. Eliane, J.-P., Repollet, M., Luker, K. E., Brown, M., Rae, J. M., Dontu, G., Schott, A. F., Wicha, M., Doyle, G. V., Hayes, D. F., and Luker, G. D. (2008) Monitoring serial changes in circulating human breast cancer cells in murine xenograft models. *Cancer Res.* **68,** 5529–5532
13. Rodenburg, W., Pennings, J. L., van Oostrom, C. T., Roodbergen, M., Kuiper, R. V., Luijten, M., and de Vries, A. (2010) Identification of breast cancer biomarkers in transgenic mouse models: a proteomics approach. *Proteomics Clin. Appl.* **4,** 603–612
14. Pitteri, S. J., Kelly-Spratt, K. S., Gurley, K. E., Kennedy, J., Buson, T. B., Chin, A., Wang, H., Zhang, Q., Wong, C.-H., Chodosh, L. A., Nelson, P. S., Hanash, S. M., and Kemp, C. J. (2011) Tumor microenvironment-derived proteins dominate the plasma proteome response during breast cancer induction and progression. *Cancer Res.* **71,** 5090–5100
15. Uotila, M., Ruoslahti, E., and Engvall, E. (1981) Two-site sandwich enzyme immunoassay with monoclonal antibodies to human alpha-fetoprotein. *J. Immunol. Methods* **42,** 11–15
16. Nielsen, U. B., and Geierstanger, B. H. (2004) Multiplexed sandwich assays in microarray format. *J. Immunol. Methods* **290,** 107–120
17. Li, H., Leulmi, R. F., and Juncker, D. (2011) Hydrogel droplet microarrays with trapped antibody-functionalized beads for multiplexed protein analysis. *Lab Chip* **11,** 528–534
18. Stoevesandt, O., and Taussig, M. J. (2012) Affinity proteomics: the role of specific binding reagents in human proteome analysis. *Expert Rev. Proteomics* **9,** 401–414
19. Yu, X., Schneiderhan-Marra, N., and Joos, T. O. (2010) Protein microarrays for personalized medicine. *Clin. Chem.* **56,** 376–387
20. Pla-Roca, M., Leulmi, R. F., Tourekhanova, S., Bergeron, S., Laforte, V., Moreau, E., Gosline, S. J. C., Bertos, N., Hallett, M., Park, M., and Juncker, D. (2012) Antibody colocalization microarray: a scalable technology for multiplex protein analysis in complex samples. *Mol. Cell. Proteomics* **11,** M111.011460
21. Juncker, D., Bergeron, S., Laforte, V., and Li, H. (2014) Cross-reactivity in antibody microarrays and multiplexed sandwich assays: shedding light on the dark side of multiplexing. *Curr. Opin. Chem. Biol.* **18,** 29–37
22. Li, H., Bergeron, S., and Juncker, D. (2012) Microarray-to-microarray transfer of reagents by snapping of two chips for cross-reactivity-free multiplex immunoassays. *Anal. Chem.* **84,** 4776–4783
23. Mourskaia, A. A., Dong, Z., Ng, S., Banville, M., Zwaagstra, J. C., O'Connor-McCourt, M. D., and Siegel, P. M. (2009) Transforming growth factor-β1 is the predominant isoform required for breast cancer cell outgrowth in bone. *Oncogene* **28,** 1005–1015
24. Wapnir, I. L., Barnard, N., Wartenberg, D., and Greco, R. S. (2001) The inverse relationship between microvessel counts and tumor volume in breast cancer. *Breast J.* **7,** 184–188
25. R&D Systems (2015) *Antibody Product Catalog*, R&D Systems, Minneapolis, MN
26. Miller, J. C., Zhou, H., Kwekel, J., Cavallo, R., Burke, J., Butler, E. B., Teh, B. S., and Haab, B. B. (2003) Antibody microarray profiling of human prostate cancer sera: antibody screening and identification of potential biomarkers. *Proteomics* **3,** 56–63
27. Grote, T., Siwak, D. R., Fritsche, H. A., Joy, C., Mills, G. B., Simeone, D., Whitcomb, D. C., and Logsdon, C. D. (2008) Validation of reverse phase protein array for practical screening of potential biomarkers in serum and plasma: Accurate detection of CA19-9 levels in pancreatic cancer. *Proteomics* **8,** 3051–3060
28. Tampellini, M., Berruti, A., Bitossi, R., Gorzegno, G., Alabiso, I., Bottini, A., Farris, A., Donadio, M., Sarobba, M. G., Manzin, E., Durando, A., Defabiani, E., De Matteis, A., Ardine, M., Castiglione, F., Danese, S., Bertone, E., Alabiso, O., Massobrio, M., and Dogliotti, L. (2006) Prognostic significance of changes in CA 15-3 serum levels during chemotherapy in metastatic breast cancer patients. *Breast Cancer Res. Treat.* **98,** 241–248
29. Shin, H., Sheu, B., Joseph, M., and Markey, M. K. (2008) Guilt-by-association feature selection: identifying biomarkers from proteomic profiles. *J. Biomed. Inform.* **41,** 124–136
30. Olsson, N., Carlsson, P., James, P., Hansson, K., Waldemarson, S., Malmström, P., Fernö, M., Ryden, L., Wingren, C., and Borrebaeck, C. A. (2013) Grading breast cancer tissues using molecular portraits. *Mol. Cell. Proteomics* **12,** 3612–3623
31. Frasci, G., Comella, P., Rinaldo, M., Iodice, G., Di Bonito, M., D'Aiuto, M., Petrillo, A., Lastoria, S., Siani, C., Comella, G., and D'Aiuto, G. (2009) Preoperative weekly cisplatin-epirubicin-paclitaxel with G-CSF support in triple-negative large operable breast cancer. *Ann. Oncol.* 20, 1185–1192
32. Kim, H., Choi, J.-A., Park, G.-S., and Kim, J.-H. (2012) BLT2 up-regulates interleukin-8 production and promotes the invasiveness of breast cancer cells. *PLoS One* **7,** e49186
33. Rody, A., Karn, T., Liedtke, C., Pusztai, L., Ruckhaeberle, E., Hanker, L., Gaetje, R., Solbach, C., Ahr, A., Metzler, D., Schmidt, M., Müller, V., Holtrich, U., and Kaufmann, M. (2011) A clinically relevant gene signature in triple negative and basal-like breast cancer. *Breast Cancer Res.* **13,** R97
34. De Larco, J. E., Wuertz, B. R., Rosner, K. A., Erickson, S. A., Gamache, D. E., Manivel, J. C., and Furcht, L. T. (2001) A potential role for interleukin-8 in the metastatic phenotype of breast carcinoma cells. *Am. J. Pathol.* **158,** 639–646
35. Fuksiewicz, M., Kowalska, M., Kotowicz, B., Rubach, M., Chechlinska, M., Pienkowski, T., and Kaminska, J. (2010) Serum soluble tumour necrosis factor receptor type I concentrations independently predict prognosis in patients with breast cancer. *Clin. Chem. Lab. Med.* **48,** 1481–1486
36. Duffy, M. J. (2004) The urokinase plasminogen activator system: role in malignancy. *Curr. Pharm. Des.* **10,** 39–49
37. Bevan, P., and Mala, C. (2008) The Role of uPA and uPA inhibitors in breast cancer. *Breast Care* **3,** Suppl. 2, 1–2
38. Neve, R. M., Chin, K., Fridlyand, J., Yeh, J., Baehner, F. L., Fevr, T., Clark, L., Bayani, N., Coppe, J.-P., Tong, F., Speed, T., Spellman, P. T., DeVries, S., Lapuk, A., Wang, N. J., Kuo, W.-L., Stilwell, J. L., Pinkel, D., Albertson, D. G., Waldman, F. M., McCormick, F., Dickson, R. B., Johnson, M. D., Lippman, M., Ethier, S., Gazdar, A., and Gray, J. W. (2006) A collection of breast cancer cell lines for the study of functionally distinct cancer subtypes. *Cancer Cell* **10,** 515–527
39. Senst, C., Nazari-Shafti, T., Kruger, S., Höner Zu Bentrup, K., Dupin, C. L., Chaffin, A. E., Srivastav, S. K., Wörner, P. M., Abdel-Mageed, A. B., Alt, E. U., and Izadpanah, R. (2013) Prospective dual role of mesenchymal stem cells in breast tumor microenvironment. *Breast Cancer Res. Treat.* **137,** 69–79
40. Yerushalmi, R., Tyldesley, S., Kennecke, H., Speers, C., Woods, R., Knight, B., and Gelmon, K. A. (2012) Tumor markers in metastatic breast cancer subtypes: frequency of elevation and correlation with outcome. *Ann. Oncol.* **23,** 338–345
41. Harris, A. L., Nicholson, S., Sainsbury, R., Wright, C., and Farndon, J. (1992) Epidermal growth factor receptor and other oncogenes as prognostic markers. *J. Natl. Cancer Inst. Monogr.* **11,** 181–187
42. Subik, K., Lee, J. F., Baxter, L., Strzepek, T., Costello, D., Crowley, P., Xing, L., Hung, M. C., Bonfiglio, T., Hicks, D. G., and Tang, P. (2010) The expression patterns of ER, PR, HER2, CK5/6, EGFR, Ki-67 and AR by immunohistochemical analysis in breast cancer cell lines. *Breast Cancer* **4,** 35–41
43. Hirsch, D. S., Shen, Y., and Wu, W. J. (2006) Growth and motility inhibition of breast cancer cells by epidermal growth factor receptor degradation is correlated with inactivation of Cdc42. *Cancer Res.* **66,** 3523–3530
44. Corkery, B., Crown, J., Clynes, M., and O'Donovan, N. (2009) Epidermal growth factor receptor as a potential therapeutic target in triple-negative breast cancer. *Ann. Oncol.* **20,** 862–867
45. Phromnoi, K., Yodkeeree, S., Anuchapreeda, S., and Limtrakul, P. (2009) Inhibition of MMP-3 activity and invasion of the MDA-MB-231 human invasive breast carcinoma cell line by bioflavonoids. *Acta Pharmacol. Sin.* **30,** 1169–1176
46. Peter, M. E., Budd, R. C., Desbarats, J., Hedrick, S. M., Hueber, A. O., Newell, M. K., Owen, L. B., Pope, R. M., Tschopp, J., Wajant, H., Wallach, D., Wiltrout, R. H., Zörnig, M., and Lynch, D. H. (2007) The CD95 receptor: apoptosis revisited. *Cell* **129,** 447–450
47. Chakrabandhu, K., Huault, S., and Hueber, A.-O. (2008) Distinctive molecular signaling in triple-negative breast cancer cell death triggered by hexadecylphosphocholine (miltefosine). *FEBS Lett.* **582,** 4176–4184
48. Riches, A. C., Sharp, J. G., Thomas, D. B., and Smith, S. V. (1973) Blood volume determination in the mouse. *J. Physiol.* **228,** 279–284
49. Finak, G., Bertos, N., Pepin, F., Sadekova, S., Souleimanova, M., Zhao, H., Chen, H., Omeroglu, G., Meterissian, S., Omeroglu, A., Hallett, M., and

Park, M. (2008) Stromal gene expression predicts clinical outcome in breast cancer. *Nat. Med.* **14,** 518–527
50. Weedon-Fekjaer, H., Lindqvist, B. H., Vatten, L. J., Aalen, O. O., and Tretli, S. (2008) Breast cancer tumor growth estimated through mammography screening data. *Breast Cancer Res.* **10,** R41
51. Tibshirani, R., Hastie, T., Narasimhan, B., and Chu, G. (2002) Diagnosis of multiple cancer types by shrunken centroids of gene expression. *Proc. Natl. Acad. Sci. U.S.A.* **99,** 6567–6572
52. Yan, Z., Li, J., Xiong, Y., Xu, W., and Zheng, G. (2012) Identification of candidate colon cancer biomarkers by applying a random forest approach on microarray data. *Oncol. Rep.* **28,** 1036–1042
53. Carlsson, A., Wingren, C., Kristensson, M., Rose, C., Fernö, M., Olsson, H., Jernström, H., Ek, S., Gustavsson, E., Ingvar, C., Ohlsson, M., Peterson, C., and Borrebaeck, C. A. (2011) Molecular serum portraits in patients with primary breast cancer predict the development of distant metastases. *Proc. Natl. Acad. Sci. U.S.A.* **108,** 14252–14257